International Journal of Engineering & Applied Sciences (IJEAS)
Vol.15, Issue 3 (2023) 125-143
http://dx.doi.org/10.24107/ijeas.1342775
Int J Eng Appl Sci 15(3) (2023) 125-143

Vibration Analysis of Porous Orthotropic Cylindrical Panels Resting on Elastic Foundations Based on Shear Deformation Theory

Ferruh Turan

Ondokuz Mayis University Faculty of Engineering Department of Civil Engineering

✉: ferruh.turan@omu.edu.tr , *: 0000-0002-4160-712X*

Received: 14.08.2023, Revised: 29.08.2023, Accepted: 19.09.2023

Abstract

Cylindrical panels are one of the most essential structural members of engineering structures, with mechanical, civil, aeronautical, and marine engineering applications. They are subjected to a wide range of vibrational loads. This article presents a novel higher-order porosity distribution and a free vibration analysis for porous orthotropic cylindrical panels resting on elastic foundations under higher-order shear deformation theory. It is assumed that cylindrical panels are composed of porous materials with uniformly and non-uniformly distributed pores. The porous panels' material properties are distributed in the thickness direction using specific functions. The equations of motion are derived using Hamilton's principle based on trigonometrical shear deformation theory and solved by performing the Galerkin solution procedure with simply supported edge conditions. The accuracy of the obtained natural frequency equation is confirmed by comparing the results to those of previously published in literature. Under comprehensive parametric studies, the influence of porosity coefficient, porosity distribution patterns, radius-to-curve length ratio, orthotropy, and stiffness of elastic foundation parameters on the free vibration response of porous orthotropic cylindrical panels are discussed in detail.

Keywords: Porous panel, vibration, shear deformation, elastic foundation, porosity.

1. Introduction

The investigation of structural components resting on elastic foundations has attracted much attention from researchers because of their application in various engineering fields, such as footings in building construction, pavements in roadways, and aeronautical engineering. A way to solve the above problems is to incorporate the elastic behavior of foundations in the equations of motion of structural components. Winkler and Pasternak's foundations are the two elastic foundation approaches considered commonly in the literature. A Winkler foundation called a one-parameter elastic foundation is represented as a separate spring. Pasternak added a shear layer over the springs to improve the assumption [1].

The mechanical behavior of structural members is analyzed using classical plate (or shell) theory, first-order shear deformation theory, and higher-order shear deformation theory. After developing these theories, many parametric studies have been carried out on the vibration problems of plates and shells resting on elastic foundations. Zamani et al. [2] analyzed the free vibration response of laminated viscoelastic composite plates resting on a Pasternak viscoelastic medium. The composite plate comprises a linear viscoelastic matrix and isotropic elastic fibers. Duc et al. [3] investigated the nonlinear dynamic and vibration problems of spherical shells made of FG material placed on an elastic foundation in the thermal environment. Material properties are graded along the thickness using a sigmoid law. Zenkour and Radwan [4] studied the free vibration of sandwich plates resting on Pasternak foundations based on hyperbolic shear deformation theory. Using Reddy's third-order shear deformation theory, Quan and Duc [5] presented the nonlinear vibration behavior of imperfect FG double-curved shells resting on an elastic foundation. They modeled the temperature-dependent material properties through the

thickness via a power-law rule. Park and Kim [6] analyzed the natural frequencies of FG cylindrical fluid-filled shells. They assumed the shells partially rested on a Pasternak elastic foundation and material properties vary along the thickness. Ninh and Bich [7] studied the nonlinear vibration characteristics of toroidal shell segments with a ceramic-FG-metal layer surrounded by an elastic foundation based on classical shell theory. Jung et al. [8] proposed a refined-higher-order shear deformation theory for analyzing the free and forced vibration of FG plates on elastic foundations. Depending on two power-law distributions, they graded the material properties in the thickness direction. Kim [9] investigated the free vibration behavior of FG cylindrical shell partially rested on elastic foundations with an oblique edge using first-order shear deformation theory. The material properties are modeled across the thickness via a four-parameter power-law. Asanjarani et al. [10] presented the influence of geometric parameters and elastic foundations on the free vibration of two-dimensional FG truncated conical shells based on the first-order shear deformation theory. The material properties are graded in the thickness and length directions using a power-law distribution. Ahmed [11] analyzed the free vibration characteristics of a non-homogeneous orthotropic elliptical cylindrical shell resting on a non-uniform Winkler foundation. Bich et al. [12] studied the nonlinear dynamic and vibration responses of imperfect eccentrically stiffened FG double-curved shells placed on elastic foundation using first-order shear deformation theory. Thai et al. [13] proposed a simple refined shear deformation theory for analyzing the bending, buckling, and vibration behaviors of thick plates resting on the Pasternak foundation. Sobhy [14] focused on the buckling and vibration of exponentially graded sandwich plates on an elastic foundation. The sandwich plate is modeled as a fully ceramic core and exponentially graded face sheets.

Porous materials play a significant role in many fields, such as energy management, vibration control, thermal insulation, and sound absorption. Porous materials such as porous metals, ceramics, and polymer foams favor various engineering applications Kamranfard et al. [15]. These superior properties of porous materials have attracted the attention of researchers. Static and dynamic behaviors of structural components made of porous materials have been studied in recent years. Turan [16] studied the free vibration response of porous orthotropic laminated plates with trigonometric porosity distribution via higher-order shear deformation theory. Wang [17] analyzed the electro-mechanical vibration of FG porous plates with porosity distribution in the thickness direction. Porous FG material properties are graded using a modified power-law rule containing the porosity effects. Rezaei and Saidi [18] presented an exact analytical approach based on the first-order shear deformation theory for free vibration analysis of fluid-saturated porous annular sector plates. They graded the material properties in the thickness direction using a cosine function. Kamranfard et al. [15] investigated the effects of porosity and geometrical parameters on the critical buckling loads and natural frequencies of moderately thick annular plates. Based on the refined shear deformation theory, Barati and Zenkour [19] studied the electro-thermoelastic vibration of FG piezoelectric porous plates. The material properties are varied along the thickness direction depending on the modified power-law rule. Using first-order shear deformation theory, Barati [20] analyzed the natural frequencies of FG porous nanoshells with porosities evenly and unevenly distributed in the thickness direction. Wang and Wu [21] presented the free vibration response of FG porous cylindrical shell under sinusoidal shear deformation theory. They considered two types of graded porosity distribution patterns across thickness. Shojaeefard et al. [22] analyzed the influence of porosity and gradation index on the free vibration and thermal buckling behavior of micro temperature-dependent FG porous plates based on the first-order shear deformation theory. Akbaş [23] investigated FG porous plates' static and vibration analysis under first-order shear deformation theory. Porosity-dependent material properties are graded in the thickness direction via a power-law model with porosities. Rezaei and Saidi [24] discussed the porosity effect on the thick plates' free vibration response using Reddy's third-order shear deformation

theory. Material properties of porous plates are determined in the thickness direction using a cosine function.

Furthermore, the literature has reported static and dynamic analysis of porous structural components on elastic foundations in recent years. Structural members on the elastic foundation are modeled depending on the Winkler and Pasternak interactions. Demir and Turan [25] investigated the critical buckling load of porous orthotropic cylindrical panels resting on the Winkler foundation. The porosity distribution is modeled in the thickness direction using a cosine function. Kumar et al. [26] analyzed the effect of porosity parameters, porosity distribution, and elastic foundation parameters on the natural frequencies of FG porous plates with variable thickness based on first-order shear deformation theory. The porosity-dependent material properties are graded using power-law, exponential-law, and sigmoid-law rules. Tran et al. [27] analyzed the static and free vibration behavior of FG porous nanoshell resting on an elastic foundation under extended four-unknown higher-order shear deformation theory. They graded the porous FG material using uneven porosity and logarithmic-uneven porosity distributions. Balak et al. [28] studied the free vibration response of an elliptical sandwich microplate made of a saturated porous core and two piezoelectric face sheets. The microplate is on the elastic foundation, and governing equations of the problem are derived using first-order shear deformation theory. Pham et al. [29] focused on the static bending and hygro-thermo-mechanical vibration behavior of porous FG sandwich double-curved shells on the elastic foundation via the four-unknown shear deformation theory. The shells comprised a full ceramic core and two porous face layers with uneven porosity distribution. Shahverdi and Barati [30] proposed a general nonlocal elasticity model to analyze the vibration of porous nanoplates resting on the elastic foundation. Material properties are modeled via a modified power-law and Mori-Tanaka models containing the porosity effects.

By reviewing the above literature, the free vibration problem of porous orthotropic cylindrical panels resting on elastic foundations has not yet been investigated. Therefore, it is of great significance to fill the gaps in the study. Based on the trigonometrical shear deformation theory, this paper focuses on the natural frequencies of porous orthotropic cylindrical panels resting on the Pasternak foundation. Porous material properties such as Young's modulus, shear modulus, and mass density vary across the thickness via trigonometric functions. The governing equations of the problem are obtained using higher-order shear deformation theory and solved via the Galerkin solution procedure. The numerical results calculated by the present frequency equation indicate good convergence and accuracy by comparing with the literature results. The effect of porosity coefficients, porosity distribution patterns, geometrical parameters, orthotropy, and elastic foundation parameters on the free vibration response of porous orthotropic cylindrical panels are discussed in detail.

2. Theoretical Formulations

Fig. 1 shows the configuration of the porous orthotropic cylindrical panel with geometrical parameters: R is the curvature radius; s, a are the length of the curve and length in the y direction, respectively; h is the thickness. The cylindrical panel resting on the elastic foundation (EF) consists of two parameters (k_s, k_w). In which k_s is Pasternak stiffness, and k_w is Winkler stiffness.

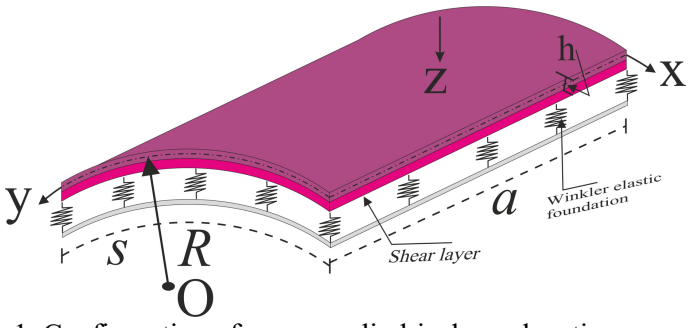

Fig. 1. Configuration of porous cylindrical panel resting on an EF

2.1. Determination of the Material Properties of the Porous Panel

This paper focuses on a non-uniform symmetric, a non-uniform asymmetric, and a uniform porosity distribution. The non-uniform symmetric porosity distribution is denoted by ND1, the non-uniform symmetric porosity distribution is abbreviated ND2, and UD indicates the uniform porosity distribution. The porosity-dependent material properties of the porous panel, including Young's modulus E, shear modulus G, and mass density ρ are varied continuously from the top surface ($z = -0.5h$) to the bottom ($z = +0.5h$) surface. The corresponding variations of material properties are given by Eqs (1)-(3) for the NDs and UD.

ND$_1$:

$$\left(E_i, G_j, \rho\right) = \left(E_{0i}, G_{0j}, \rho_0\right)\left(1 - [\eta_0, \eta_0, \eta_0^*]\right)\frac{3.45}{\pi} sin^2\left(\frac{\pi z}{h}\right), i = 1,2; j = 12, 13, 23 \quad (1a)$$

ND$_2$:

$$\left(E_i, G_j, \rho\right) = \left(E_{0i}, G_{0j}, \rho_0\right)\left(1 - [\eta_0, \eta_0, \eta_0^*]\right)\frac{3.45}{\pi} sin\left(\frac{\pi z}{h}\right), i = 1,2; j = 12, 13, 23 \quad (1b)$$

UD:

$$\left(E_i, G_j, \rho\right) = \left(E_{0i}, G_{0j}, \rho_0\right)[\hat{\eta}_0, \hat{\eta}_0, \hat{\eta}_0^*], i = 1,2; j = 12, 13, 23 \quad (1c)$$

where $0 \leq \eta_0, \hat{\eta}_0, \eta_0^*, \hat{\eta}_0^* < 1$ is the porosity coefficients and E_0, G_0 and ρ_0 are corresponding values of the material with no porosity ($\eta_0 = 0$). The porous panel's Poisson ratio (ν_{12}) is assumed to be constant along the panel thickness. Fig. 2 presents the difference between the non-uniform symmetric porosity distribution (*ND*$_1$) with the non-uniform asymmetric distribution (*ND*$_2$).

The typical mechanical properties of porous material in terms of mass density can be given as follows [31]

$$E_{max}/E_{min} = (\rho_{max}/\rho_{min})^2 \quad (2)$$

According to $\eta_0 = 1 - E_i/E_{0i}$ and $\eta_0^* = 1 - \rho/\rho_0$, the following relation can be obtained using Eq. (2):

$$\eta_0^* = 1 - \sqrt{1 - \eta_0}, \qquad \hat{\eta}_0^* = \sqrt{\hat{\eta}_0} \quad (3a)$$

Without loss of generality, the UD and ND_1 porous panels' masses are set to be equal, and the relationship between $\hat{\eta}_0$ and η_0 can be estimated using the following equation:

$$\hat{\eta}_0 = -2.7379\eta_0^6 + 6.9529\eta_0^5 - 7.0465\eta_0^4 + 3.5157\eta_0^3 - 0.9543\eta_0^2 - 0.4356\eta_0 + 0.9949 \tag{3b}$$

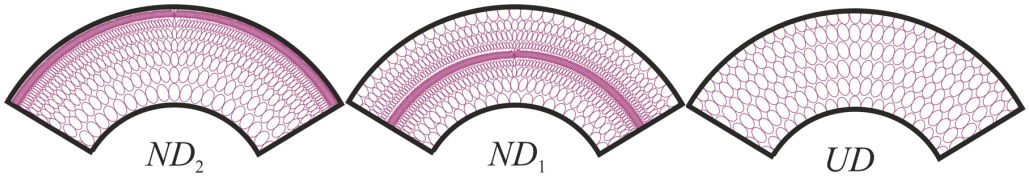

(a)

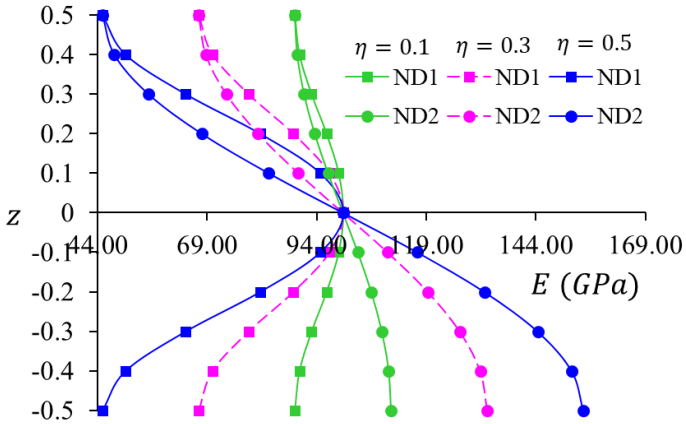

(b)

Fig. 2. (a) Three types of the porosity distribution patterns of porous material, (b) variation of Young's modulus (E_1) of the non-uniform symmetric and non-uniform asymmetric porosity distributions along the thickness direction

2.2. Kinematic Relations

This section contains the derivation of the cylindrical panel's kinematic relations. A cylindrical panel's displacement fields can be expressed based on the higher-order shear deformable plate theory as follows:

$$\begin{aligned} u_x(x,y,z,t) &= u_1(x,y,t) - zu_{3,x} + \phi(z)\Gamma_x(x,y,t) \\ u_y(x,y,z,t) &= u_2(x,y,t) - zu_{3,y} + \phi(z)\Gamma_y(x,y,t) \\ u_z(x,y,z,t) &= u_3(x,y,t) \end{aligned} \tag{4}$$

where u_1 and u_2 are longitudinal and transverse displacements of the mid-surface, respectively; u_3 is the deflection through the z-axis. Γ_x and Γ_y are the rotations of the cross-section about the y- and x-axis, respectively. $\phi(z)$ represents the shape function of shear deformation theory. The following equation defines the nonzero strains of the panel:

$$\varepsilon_{xx} = \varepsilon_{xx}^0 - z\varepsilon_{xx}^1 + \phi(z)\varepsilon_{xx}^2, \varepsilon_{yy} = \varepsilon_{yy}^0 - z\varepsilon_{yy}^1 + \phi(z)\varepsilon_{yy}^2 \tag{5}$$

$$\gamma_{xy} = \gamma_{xy}^0 - z\gamma_{xy}^1 + \phi(z)\gamma_{xy}^2, \gamma_{xz} = \varphi(z)\Gamma_x(x,y,t), \gamma_{yz} = \varphi(z)\Gamma_y(x,y,t)$$

where

$$\begin{aligned} &\varepsilon_{xx}^0 = u_{1,x} - u_3\hat{R}, \varepsilon_{yy}^0 = u_{2,y}, \gamma_{xy}^0 = u_{1,y} + u_{2,x} \\ &\varepsilon_{xx}^1 = u_{3,xx}, \varepsilon_{yy}^1 = u_{3,yy}, \varepsilon_{xy}^1 = 2u_{3,xy} \\ &\varepsilon_{xx}^2 = \Gamma_{x,x}, \varepsilon_{yy}^2 = \Gamma_{y,y}, \varepsilon_{xy}^2 = \Gamma_{x,y} + \Gamma_{y,x} \\ &\varphi(z) = \phi_{,z}(z), \hat{R} = 1/R \end{aligned} \tag{6}$$

In this paper, the following shape function is considered by Ebrahimi et al. [32]:

$$\phi(z) = \frac{he^z}{h^2+\pi^2}\left(\pi sin\left(\frac{\pi z}{h}\right) + hcos\left(\frac{\pi z}{h}\right)\right) - \frac{h^2}{h^2+\pi^2} \tag{7}$$

2.3. Equations of Motion

Here, Hamilton's principle can be performed to reach the Euler–Lagrange equations of a porous orthotropic cylindrical panel. This principle can be defined in the following form:

$$\int_{t_1}^{t_2} \left(\delta u_s + \delta u_f - \delta u_k\right) dt = 0 \tag{8}$$

where δu_s, δu_f and δu_k are strain energy, elastic foundation's potential energy, and kinetic energy, respectively. The variation of strain energy can be expressed as

$$\begin{aligned} \delta u_s &= \int_V^0 \left(\sigma_{xx}\delta\varepsilon_{xx} + \sigma_{yy}\delta\varepsilon_{yy} + \tau_{xy}\delta\gamma_{xy} + \tau_{xz}\delta\gamma_{xz} + \tau_{yz}\delta\gamma_{yz}\right) dV \\ &= \int_0^a \int_0^b \begin{pmatrix} N_{xx}\delta\varepsilon_{xx}^0 + N_{yy}\delta\varepsilon_{yy}^0 + N_{xy}\delta\gamma_{xy}^0 + M_{xx}\delta\varepsilon_{xx}^1 + M_{yy}\delta\varepsilon_{yy}^1 + M_{xy}\delta\gamma_{xy}^1 \\ +P_{xx}\delta\varepsilon_{xx}^2 + P_{yy}\delta\varepsilon_{yy}^2 + P_{xy}\delta\gamma_{xy}^2 + N_{xz}\varepsilon_{xx}^2 + N_{yz}\varepsilon_{yy}^2 \end{pmatrix} dxdy \end{aligned} \tag{9}$$

In Eq. (9), the axial forces, bending moments, higher-order moments, and shear forces can be defined as:

$$\begin{aligned} (N_i, M_i, P_i) &= \int_{-0.5h}^{0.5h} (1, z, \phi(z))\sigma_i \, , i = xx, yy, \\ \left(N_j, M_j, P_j\right) &= \int_{-0.5h}^{0.5h} (1, z, \phi(z))\tau_j \, , j = xy, \end{aligned} \tag{10}$$

$$N_k = \int_{-0.5h}^{0.5h} \varphi(z)\tau_k \, , k = xz, yz$$

The variation of the elastic foundation's potential energy can be determined as:

$$\delta u_f = \int_0^a \int_0^b \left(k_w u_3 - k_s\left(u_{3,xx} + u_{3,yy}\right)\right) \delta u_3 \, dxdy \tag{11}$$

The first variation of kinetic energy can be expressed as:

$$\begin{aligned} \delta u_k &= \int_V \rho\left(\dot{u}_x \delta \dot{u}_x + \dot{u}_y \delta \dot{u}_y + \dot{u}_z \delta \dot{u}_z\right) dV \\ &= I_0 \int_0^a \int_0^b (\dot{u}_1 \delta \dot{u}_1 + \dot{u}_2 \delta \dot{u}_2 + \dot{u}_3 \delta \dot{u}_3) dxdy + I_1 \int_0^a \int_0^b \left(\dot{u}_{3,x} \delta \dot{u}_{3,x} + \dot{u}_{3,y} \delta \dot{u}_{3,y}\right) dxdy \\ &+ I_2 \int_0^a \int_0^b \left(\dot{\Gamma}_{x,x} \delta \dot{\Gamma}_{x,x} + \dot{\Gamma}_{y,y} \delta \dot{\Gamma}_{y,y}\right) dxdy \end{aligned} \tag{12}$$

In all the equations, the dot-superscript denotes the differentiation with respect to time, and the mass inertias used in the above equations are given in the following form:

$$(I_0, I_1, I_2) = \int_{-0.5h}^{0.5h} \rho(1, z^2, [\phi(z)]^2) dz \tag{13}$$

By substituting Eqs. (9), (11), and (12) into Eq. (8) and setting the coefficients of δu_1, δu_2, δu_3, $\delta \Gamma_x$, and $\delta \Gamma_y$ to zero, the Euler–Lagrange equations of porous orthotropic cylindrical panels can be obtained as:

$$N_{xx,x} + N_{xy,y} = I_0 \ddot{u}_1 \tag{14a}$$

$$N_{xy,x} + N_{yy,y} = I_0 \ddot{u}_2 \tag{14b}$$

$$\begin{aligned} \hat{R} N_{xx} + M_{xx,xx} + 2M_{xy,xy} + M_{yy,yy} - k_w u_3 + k_s\left(u_{3,xx} + u_{3,yy}\right) \\ = I_0 \ddot{u}_3 - I_1\left(\ddot{u}_{3,xx} + \ddot{u}_{3,yy}\right) \end{aligned} \tag{14c}$$

$$P_{xx,x} + P_{xy,y} - N_{xz} = I_2 \ddot{\Gamma}_x \tag{14d}$$

$$P_{xy,x} + P_{yy,y} - N_{yz} = I_2 \ddot{\Gamma}_y \tag{14e}$$

The inertial forces $I_0 \ddot{u}_1$ and $I_0 \ddot{u}_2$are assumed to be negligible in light of the assumption of $(u_1, u_2) \ll u_3$. By deriving Eqs. (14a) and (14d) with respect to x, and Eqs. (14b) and (14e) with respect to y gives us:

$$N_{xx,xx} + N_{xy,xy} = 0 \tag{15a}$$

$$N_{xy,xy} + N_{yy,yy} = 0 \tag{15b}$$

$$\begin{aligned}\hat{R}N_{xx} + M_{xx,xx} + 2M_{xy,xy} + M_{yy,yy} - k_w u_3 + k_s\left(u_{3,xx} + u_{3,yy}\right) \\ = I_0\ddot{u}_3 - I_1\left(\ddot{u}_{3,xx} + \ddot{u}_{3,yy}\right)\end{aligned} \tag{15c}$$

$$P_{xx,xx} + P_{xy,xy} - N_{xz,x} = I_2\ddot{\Gamma}_{x,x} \tag{15d}$$

$$P_{xy,xy} + P_{yy,yy} - N_{yz,y} = I_2\ddot{\Gamma}_{y,y} \tag{15e}$$

2.4. Stress-Strain Relations

The stress-strain relations of a porous orthotropic cylindrical panel can be written as the following equation using Hooke's law.

$$\begin{gathered}\sigma_{xx} = e_{11}\varepsilon_{xx} + e_{12}\varepsilon_{yy};\ \sigma_{yy} = e_{12}\varepsilon_{xx} + e_{22}\varepsilon_{yy};\ \tau_{yz} = e_{44}\gamma_{yz};\ \tau_{xz} = e_{55}\gamma_{xz};\\ \tau_{xy} = e_{66}\gamma_{xy}\end{gathered} \tag{16}$$

where

$$\begin{gathered}e_{11} = \frac{E_1}{1-\nu_{12}\nu_{21}}, e_{12} = \frac{\nu_{21}E_1}{1-\nu_{12}\nu_{21}}, e_{22} = \frac{E_2}{1-\nu_{12}\nu_{21}}, e_{44} = G_{23}, e_{55} = G_{13},\\ e_{66} = G_{12}\end{gathered} \tag{17}$$

Substituting Eqs. (5), (6), and (16) into Eq. (10) gives the following equation:

$$\begin{aligned}N_{xx} &= A_{11}u_{1,x} + A_{12}u_{2,y} - B_{11}u_{3,xx} - B_{12}u_{3,yy} + C_{11}\Gamma_{x,x} + C_{12}\Gamma_{y,y}\\ N_{yy} &= A_{12}u_{1,x} + A_{22}u_{2,y} - B_{12}u_{3,xx} - B_{22}u_{3,yy} + C_{12}\Gamma_{x,x} + C_{22}\Gamma_{y,y}\\ N_{xy} &= A_{66}u_{1,y} + A_{66}u_{2,x} - 2B_{66}u_{3,xy} + C_{66}\Gamma_{x,y} + C_{66}\Gamma_{y,x}\end{aligned} \tag{18a}$$

$$\begin{aligned}M_{xx} &= B_{11}u_{1,x} + B_{12}u_{2,y} - D_{11}u_{3,xx} - D_{12}u_{3,yy} + E_{11}\Gamma_{x,x} + E_{12}\Gamma_{y,y}\\ M_{yy} &= B_{12}u_{1,x} + B_{22}u_{2,y} - D_{12}u_{3,xx} - D_{22}u_{3,yy} + E_{12}\Gamma_{x,x} + E_{22}\Gamma_{y,y}\\ M_{xy} &= B_{66}u_{1,y} + B_{66}u_{2,x} - 2D_{66}u_{3,xy} + E_{66}\Gamma_{x,y} + E_{66}\Gamma_{y,x}\end{aligned} \tag{18b}$$

$$\begin{aligned}P_{xx} &= C_{11}u_{1,x} + C_{12}u_{2,y} - E_{11}u_{3,xx} - E_{12}u_{3,yy} + F_{11}\Gamma_{x,x} + F_{12}\Gamma_{y,y}\\ P_{yy} &= C_{12}u_{1,x} + C_{22}u_{2,y} - E_{12}u_{3,xx} - E_{22}u_{3,yy} + F_{12}\Gamma_{x,x} + F_{22}\Gamma_{y,y}\\ P_{xy} &= C_{66}u_{1,y} + C_{66}u_{2,x} - 2E_{66}u_{3,xy} + F_{66}\Gamma_{x,y} + F_{66}\Gamma_{y,x}\end{aligned} \tag{18c}$$

$$\begin{aligned}N_{xz} &= D_{55}\Gamma_x\\ N_{yz} &= D_{44}\Gamma_y\end{aligned} \tag{18d}$$

in which

$$[A_i, B_i, C_i, D_i, E_i, F_i] = \int_{-0.5h}^{0.5h} [1, z, \phi(z), z^2, z\phi(z), [\phi(z)]^2]e_i dz\,, i = 11,12,22,66 \tag{19}$$

$$[D_j] = \int_{-0.5h}^{0.5h} [\varphi(z)]^2 e_j dz\,, j = 44{,}55$$

2.5. Governing Equations

The inertial forces caused by Γ_x and Γ_y rotations in Eqs. (15d) and (15e) are minimal, so they are negligible. Substituting Eq. (18) into Eq. (15) gives the following partial differential governing equations:

$$\begin{aligned} &A_{11}u_{1,xxx} + A_{66}u_{1,xyy} + (A_{12} + A_{66})u_{2,xxy} - B_{11}u_{3,xxxx} - (B_{12} + 2B_{66})u_{3,xxyy} \\ &\quad + C_{11}\Gamma_{x,xxx} + C_{66}\Gamma_{x,xyy} + (C_{12} + C_{66})\Gamma_{y,xxy} = 0 \end{aligned} \tag{20a}$$

$$\begin{aligned} &(A_{12} + A_{66})u_{1,xyy} + A_{22}u_{2,yyy} + A_{66}u_{2,xxy} - (B_{12} + 2B_{66})u_{3,xxyy} - B_{22}u_{3,yyyy} \\ &\quad + (C_{12} + C_{66})\Gamma_{x,xyy} + C_{22}\Gamma_{y,yyy} + C_{66}\Gamma_{y,xxy} = 0 \end{aligned} \tag{20b}$$

$$\begin{aligned} &B_{11}u_{1,xxx} + (B_{12} + 2B_{66})\left(u_{1,xyy} + u_{2,xxy}\right) + B_{22}u_{2,yyy} - D_{11}u_{3,xxxx} \\ &\quad - 2(D_{12} + 2D_{66})u_{3,xxyy} - D_{22}u_{3,yyyy} + E_{11}\Gamma_{x,xxx} \\ &\quad + (E_{12} + 2E_{66})\left(\Gamma_{x,xyy} + \Gamma_{y,xxy}\right) + E_{22}\Gamma_{y,yyy} \\ &\quad + \hat{R}\left(A_{11}u_{1,x} + A_{12}u_{2,y} - B_{11}u_{3,xx} - B_{12}u_{3,yy} + C_{11}\Gamma_{x,x} + C_{12}\Gamma_{y,y}\right) \\ &\quad - k_w u_3 + k_s\left(u_{3,xx} + u_{3,yy}\right) - I_0\ddot{u}_3 + I_1\left(\ddot{u}_{3,xx} + \ddot{u}_{3,yy}\right) = 0 \end{aligned} \tag{20c}$$

$$\begin{aligned} &C_{11}u_{1,xxx} + C_{66}u_{1,xyy} + (C_{12} + C_{66})u_{2,xxy} - E_{11}u_{3,xxxx} - (E_{12} + 2E_{66})u_{3,xxyy} \\ &\quad + F_{11}\Gamma_{x,xxx} + F_{66}\Gamma_{x,xyy} + (F_{12} + F_{66})\Gamma_{y,xxy} - D_{55}\Gamma_{x,x} = 0 \end{aligned} \tag{20d}$$

$$\begin{aligned} &(C_{12} + C_{66})u_{1,xyy} + C_{22}u_{2,yyy} + C_{66}u_{2,xxy} - (E_{12} + 2E_{66})u_{3,xxyy} - E_{22}u_{3,yyyy} \\ &\quad + (F_{12} + F_{66})\Gamma_{x,xyy} + F_{22}\Gamma_{y,yyy} + F_{66}\Gamma_{y,xxy} - D_{44}\Gamma_{y,y} = 0 \end{aligned} \tag{20e}$$

3. Solution Technique

Here, an analytical solution of the governing equations for free vibration of a porous orthotropic cylindrical panel with simply supported edges is presented. The boundary conditions for simply supported edges are given as follows:

$$\begin{aligned} u_3 = M_{xx} = \Gamma_y = 0 \;\; at \;\; x = 0, a \\ u_3 = M_{yy} = \Gamma_x = 0 \;\; at \;\; y = 0, b \end{aligned} \tag{21}$$

The displacement fields are presented in the following form to satisfy the above boundary conditions:

$$\begin{aligned} u_1 = u_{11}cos(\lambda_1 x)\, sin(\lambda_2 y)\, e^{i\omega t}, u_2 = u_{22}sin\,(\lambda_1 x)cos\,(\lambda_2 y)e^{i\omega t} \\ u_3 = u_{33}sin(\lambda_1 x)\, sin(\lambda_2 y)\, e^{i\omega t}, \Gamma_x = u_{44}cos\,(\lambda_1 x)sin\,(\lambda_2 y)e^{i\omega t} \end{aligned} \tag{22}$$

$$\Gamma_y = u_{55} sin\,(\lambda_1 x) cos\,(\lambda_2 y) e^{i\omega t}$$

where (u_{11}, u_{22}, u_{33}, u_{44}, u_{55}) are the unknown coefficients ($\lambda_1 = m\pi/s$, $\lambda_2 = n\pi/a$). Substituting Eq. (22) into Eq. (20) and then utilizing the Galerkin solution procedure leads to:

$$\begin{aligned}
&K_{11}u_{11} + K_{12}u_{22} + K_{13}u_{33} + K_{14}u_{44} + K_{15}u_{55} = 0\\
&K_{21}u_{11} + K_{22}u_{22} + K_{23}u_{33} + K_{24}u_{44} + K_{25}u_{55} = 0\\
&K_{31}u_{11} + K_{32}u_{22} + K_{33}u_{33} + K_{34}u_{44} + K_{35}u_{55} - \widehat{K}_{33}\omega^2 u_{33} = 0\\
&K_{41}u_{11} + K_{42}u_{22} + K_{43}u_{33} + K_{44}u_{44} + K_{45}u_{55} = 0\\
&K_{51}u_{11} + K_{52}u_{22} + K_{53}u_{33} + K_{54}u_{44} + K_{55}u_{55} = 0
\end{aligned} \tag{23}$$

where

$$K_{11} = \frac{sa}{4}(\lambda_1^3 A_{11} + \lambda_1\lambda_2^2 A_{66});\ K_{12} = \frac{sa}{4}\lambda_1^2\lambda_2(A_{12} + A_{66});$$

$$K_{13} = -\frac{sa}{4}\left(\lambda_1^4 B_{11} + \lambda_1^2\lambda_2^2(B_{12} + 2B_{66})\right);\ K_{14} = \frac{sa}{4}(\lambda_1^3 C_{11} + \lambda_1\lambda_2^2 C_{66});$$

$$K_{15} = \frac{sa}{4}\lambda_1^2\lambda_2(C_{12} + C_{66});\ K_{21} = \frac{sa}{4}\lambda_1\lambda_2^2(A_{12} + A_{66});$$

$$K_{22} = \frac{sa}{4}(\lambda_1^2\lambda_2 A_{66} + \lambda_2^3 A_{22});\ K_{23} = -\frac{sa}{4}(\lambda_1^2\lambda_2^2(B_{12} + 2B_{66}) + \lambda_2^4 B_{22});$$

$$K_{24} = \frac{sa}{4}\lambda_1\lambda_2^2(C_{12} + C_{66});\ K_{25} = \frac{sa}{4}(\lambda_1^2\lambda_2 C_{66} + \lambda_2^3 C_{22});$$

$$K_{31} = \frac{sa}{4}\left(\lambda_1^3 B_{11} + \lambda_1\lambda_2^2(B_{12} + 2B_{66}) - \lambda_1 A_{11}\hat{R}\right);$$

$$K_{32} = \frac{sa}{4}\left(\lambda_1^2\lambda_2(B_{12} + 2B_{66}) + \lambda_2^3 B_{22} - \lambda_2 A_{12}\hat{R}\right);$$

$$\begin{aligned}
K_{33} = -\frac{sa}{4}\Big(&\lambda_1^4 D_{11} + 2\lambda_1^2\lambda_2^2(D_{12} + 2D_{66}) + \lambda_2^4 D_{22} - (\lambda_1^2 B_{11} + \lambda_2^2 B_{12})\hat{R} + k_w\\
&+ k_s(\lambda_1^2 + \lambda_2^2)\Big);\ K_{34} = \frac{sa}{4}\left(\lambda_1^3 E_{11} + \lambda_1\lambda_2^2(E_{12} + 2E_{66}) - \lambda_1 C_{11}\hat{R}\right);
\end{aligned} \tag{24}$$

$$K_{35} = \frac{sa}{4}\left(\lambda_1^2\lambda_2(E_{12} + 2E_{66}) + \lambda_2^3 E_{22} - \lambda_2 C_{12}\hat{R}\right);$$

$$\widehat{K}_{33} = -\frac{sa}{4}\left(I_0 + I_1(\lambda_1^2 + \lambda_2^2)\right);\ K_{41} = \frac{sa}{4}(\lambda_1^3 C_{11} + \lambda_1\lambda_2^2 C_{66});$$

$$K_{42} = \frac{sa}{4}\lambda_1^2\lambda_2(C_{12} + C_{66});\ K_{43} = -\frac{sa}{4}\left(\lambda_1^4 E_{11} + \lambda_1^2\lambda_2^2(E_{12} + 2E_{66})\right);$$

$$K_{44} = \frac{sa}{4}(\lambda_1^3 F_{11} + \lambda_1\lambda_2^2 F_{66} + \lambda_1 D_{55});\ K_{45} = \frac{sa}{4}\lambda_1^2\lambda_2(F_{12} + F_{66});$$

$$K_{51} = \frac{sa}{4}\lambda_1\lambda_2^2(C_{12} + C_{66});\ K_{52} = \frac{sa}{4}(\lambda_1^2\lambda_2 C_{66} + \lambda_2^3 C_{22});$$

$$K_{53} = -\frac{sa}{4}(\lambda_1^2\lambda_2^2(E_{12} + 2E_{66}) + \lambda_2^4 E_{22});\ K_{54} = \frac{sa}{4}\lambda_1\lambda_2^2(F_{12} + F_{66});$$

$$K_{55} = \frac{sa}{4}(\lambda_1^2\lambda_2 F_{66} + \lambda_2^3 F_{22} + \lambda_2 D_{44})$$

By obtaining the determinant of the coefficient matrix of the following equation and setting this multinomial to zero, we can obtain Eq. (26):

$$\begin{bmatrix} K_{11} & K_{12} & K_{13} & K_{14} & K_{15} \\ K_{21} & K_{22} & K_{23} & K_{24} & K_{25} \\ K_{31} & K_{32} & K_{33}-\omega^2\widehat{K}_{33} & K_{34} & K_{35} \\ K_{41} & K_{42} & K_{43} & K_{44} & K_{45} \\ K_{51} & K_{52} & K_{53} & K_{54} & K_{55} \end{bmatrix} \begin{Bmatrix} u_{11} \\ u_{22} \\ u_{33} \\ u_{44} \\ u_{55} \end{Bmatrix} = 0 \tag{25}$$

$$K_{31}\alpha_{31} + K_{32}\alpha_{32} + \left(K_{33} - \omega^2\widehat{K}_{33}\right)\alpha_{33} + K_{34}\alpha_{34} + K_{35}\alpha_{35} = 0 \tag{26}$$

where $\alpha_{3j}(j = 1,2,..,5)$ are cofactors of the matrix in Eq. (25) and are presented in Appendix A. The porous orthotropic cylindrical panel's natural frequency can be obtained as follows:

$$\omega = \sqrt{(K_{31}\alpha_{31} + K_{32}\alpha_{32} + K_{33}\alpha_{33} + K_{34}\alpha_{34} + K_{35}\alpha_{35})/\widehat{K}_{33}\alpha_{33}} \tag{27}$$

4. Numerical Results and Discussions

In this section, the results are validated by comparing the obtained results with those of isotropic plates resting on the Pasternak foundation reported by Akhavan et al. [33] in Table 1 and those of porous isotropic cylindrical panel presented by Talebizadehsardari et al. [34] in Table 2. Then, the effect of porosity coefficients, porosity distribution patterns, orthotropy, geometrical parameters, and EF stiffness on the natural frequencies of porous orthotropic cylindrical panels resting on EF will be investigated. The non-dimensional parameters can be given as the relation in Eq. (28):

$$\widehat{\omega} = \omega s^2\sqrt{\rho_0 h/D_0};\ D_0 = E_1 h^3/12(1-\nu_{12}\nu_{21});\ \hat{k}_w = k_w s^4/D_0;\ \hat{k}_s = k_s s^2/D_0 \tag{28}$$

By studying Tables 1-2, it is found that the non-dimensional natural frequencies obtained in the present study are in good agreement with the results reported in the literature and thus validate the proposed solution method.

Table 1. The fundamental frequency $\widehat{\omega}$ for isotropic ($\nu_{12} = \nu_{21} = 0.3$) square plate ($\hat{R} \to 0$).

	$\hat{k}_w, \hat{k}_s$					
	Akhavan et al. [33]			Present		
s/h	(0,0)	$(10^2, 10^1)$	$(10^3, 10^2)$	(0,0)	$(10^2, 10^1)$	$(10^3, 10^2)$
5	17.5055	24.3074	56.0359	17.1126	23.9139	55.5262
10	18.0840	25.6368	57.3969	19.0415	25.5961	57.3444
1000	19.7391	26.2112	57.9961	19.7426	26.2138	57.9973

Table 2. The fundamental natural frequency $\bar{\omega} = (\omega a^2/h)\sqrt{\rho/E}$ for the *UD* cylindrical panels ($E = 70\ GPa, \nu = 0.3, \rho = 2702\ kg/m^3\ , h = 0.2\ m, R = 1.93\ m, s = 1.011\ m, a = 1\ m$).

η_0	Talebizadehsardari et al. [34]	Present
0	5.3650	5.3598
0.2	5.1815	5.2104
0.4	4.9651	5.0314

4.1. Natural Vibration Analysis

The following study analyzes the natural vibration of the porous orthotropic cylindrical panel with three porosity distribution patterns. The material properties of the orthotropic cylindrical panel are selected as $E_{01} = 53.78\ GPa$, $E_{02} = 17.93\ GPa$, $G_{012} = G_{013} = 8.96\ GPa$, $G_{023} = 3.45\ GPa$, $\nu_{12} = 0.25$, $\rho_0 = 1900\ kgm^{-3}$.

Table 3 and Fig. 4 report the non-dimensional fundamental natural frequencies of porous orthotropic cylindrical panels with various porosity coefficients, EF stiffness, and porosity distribution patterns at $s/h = 50$, $s/a = 1$, $R/s = 5$. The fundamental natural frequency decreases with increasing porosity coefficient for all porosity distribution patterns. The enormous and minor frequencies are obtained for ND_2 and ND_1 patterns. The most significant porosity effect is obtained in ND_1 cylindrical panels. With increasing porosity coefficient from 0 to 0.9, the ND_1 pattern effect on the fundamental natural frequencies increases as (27%), (16%), and (7.5%) for no foundation, Winkler foundation, and Pasternak foundation, respectively. With an increasing porosity coefficient from 0 to 0.9 at no foundation case, the ND_1 pattern effect on the fundamental natural frequencies increases (12%) and (16%) compared to the *UD* and ND_2 patterns.

Table 3. Variation of cylindrical panel's non-dimensional fundamental natural frequency with different foundation parameters, porosity coefficient, and distribution patterns.

	$\hat{k}_w, \hat{k}_s$								
	0,0			60,0			60,4		
η_0	UD	ND_1	ND_2	UD	ND_1	ND_2	UD	ND_1	ND_2
0	17.904	17.904	17.904	19.507	19.507	19.507	21.434	21.434	21.434
0.1	17.651	17.453	17.964	19.320	19.139	19.562	21.318	21.154	21.484
0.2	17.383	16.977	17.935	19.125	18.758	19.535	21.201	20.872	21.460
0.3	17.095	16.471	17.816	18.921	18.362	19.426	21.085	20.588	21.361
0.4	16.786	15.932	17.606	18.708	17.952	19.233	20.970	20.306	21.185
0.5	16.447	15.355	17.300	18.481	17.528	18.954	20.858	20.032	20.932
0.6	16.070	14.735	16.895	18.240	17.096	18.585	20.751	19.777	20.599
0.7	15.644	14.067	16.382	17.980	16.663	18.120	20.655	19.561	20.180
0.8	15.131	13.352	15.750	17.689	16.260	17.550	20.576	19.434	19.670
0.9	14.415	12.626	14.984	17.329	15.983	16.867	20.543	19.540	19.063

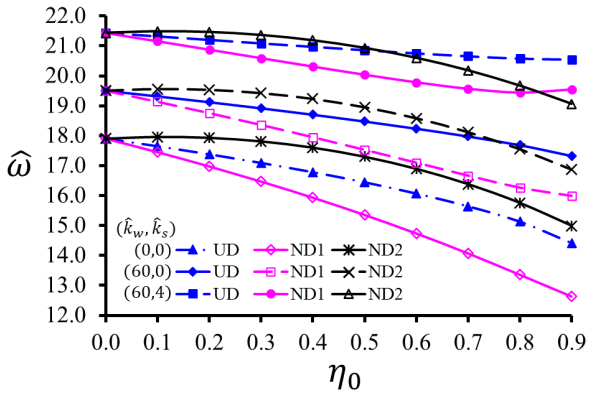

Fig. 4. Variation of non-dimensional fundamental frequency versus porosity coefficients for various elastic foundation stiffness

In the same case, the most significant ND_2 pattern effect is (5.2%) compared to the *UD* pattern at $\eta_0 = 0.5$. Depending on the rising porosity coefficient from 0 to 0.9, the Winkler foundation effect on the fundamental natural frequencies increases (11.3%), (17.6%), and (3.6%) for *UD*, ND_1, and ND_2 patterns, respectively. In the same case, the influence of the Pasternak foundation increases (22.8%), (35%), and (7.5%) for *UD*, ND_1, and ND_2 patterns, respectively.

Figs. 5 and 6 indicate the variation of the dimensionless fundamental natural frequency of porous orthotropic cylindrical panel resting on the Winkler and Pasternak foundations for different porosity coefficients and three porosity distributions at ($s/h = 50$, $s/a = 1$, $R/s = 5$). It is known that the growth of Winkler and Pasternak stiffness leads to increasing in dimensionless fundamental frequency for all porosity coefficients. Moreover, it is found that the effect of porosity on fundamental frequencies is more considerable with no elastic foundation. In other words, the influence of porosity decreases with increasing foundation stiffness. With an increasing Winkler foundation stiffness from 0 to 150 at $\eta_0 = 0.6$, the porosity effect diminishes as (7.4%), (10.5%), and (1.4%) for *UD, ND*$_1$, *and ND*$_2$ patterns, respectively. With an increasing Pasternak foundation stiffness from 0 to 15 at $\eta_0 = 0.8$, the porosity effect decreases as (6.8%), (17.2%), and (4.7%) for UD, ND$_1$, *and* ND$_2$ *patterns*, respectively. With an increasing Pasternak foundation stiffness from 0 to 15 at $\eta_0 = 0.8$, the ND$_1$ pattern effect on the fundamental natural frequencies diminishes as (6%) compared to the UD pattern. It decreases by (8.5%) and then increases by (6.6%) compared to the ND$_2$ pattern. Depending on the increase in the foundation stiffness, the effect of the elastic foundation on the dimensional fundamental frequencies increases as expected.

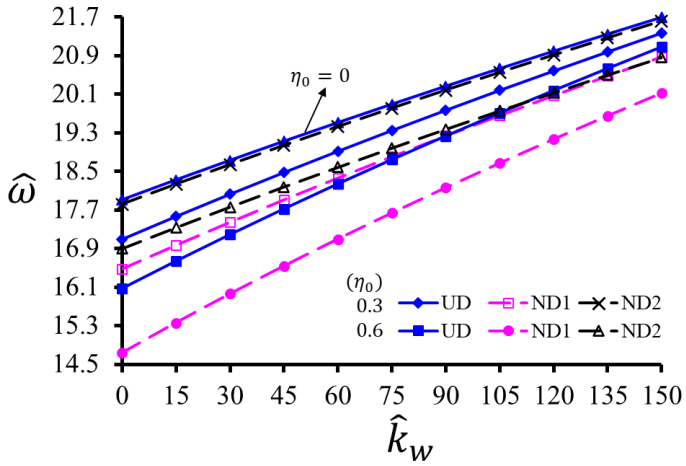

Fig. 5. Variation of non-dimensional fundamental frequency versus Winkler elastic foundation stiffness for various porosity coefficients

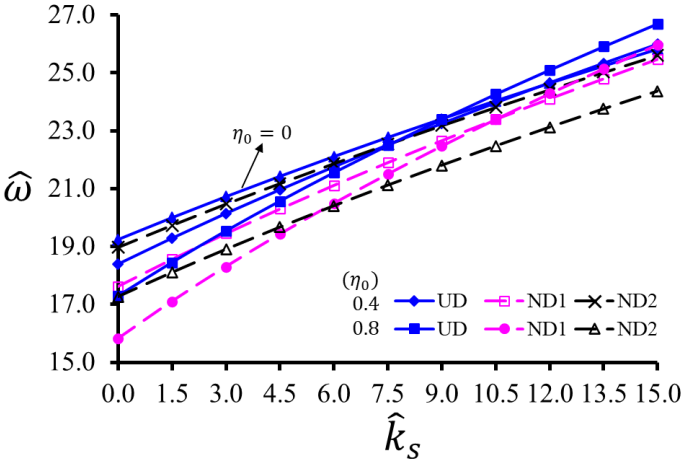

Fig. 6. Variation of non-dimensional fundamental frequency versus Pasternak elastic foundation stiffness for various porosity coefficients

Fig. 7 and Table 4 show the influence of in-plane orthotropy on the free vibration behavior of porous orthotropic cylindrical panel resting on elastic foundation with respect to three porosity distributions at ($s/h = 50$, $s/a = 1$, $R/s = 5$). With an increasing orthotropy ratio from 5 to

60 at no foundation case, the porosity effect increases by (2.4%) and (5.4%) for ND_1 *and* ND_2 patterns, respectively. It remains constant at (8%) for the *UD* pattern. With an increasing orthotropy ratio from 5 to 60 at the Pasternak foundation case, the porosity effect diminishes by (1.6%) and (3.6%) for *UD and* ND_1 patterns, respectively. It increases by (1.7%) for the ND_2 pattern. With an increasing orthotropy ratio from 5 to 60 at the Pasternak foundation case, the ND_1 pattern effect on the fundamental natural frequencies diminishes by (1.5%) compared to the *UD* pattern. It decreases by (3.3%) and then increases by (2%) compared to the ND_2 pattern. Depending on the rising orthotropy ratio from 5 to 60, the Pasternak foundation effect on the fundamental natural frequencies increases (28%), (34.5%), and (28%) for *UD*, ND_1, and ND_2 patterns, respectively.

Table 4. The effect of orthotropy on the cylindrical panel's non-dimensional fundamental natural frequency with different foundation parameters, porosity coefficient, and distribution patterns.

	$\eta_0 = 0$		$\eta_0 = 0.5$					
	$\hat{k}_w, \hat{k}_s$							
	0,0	100,0.4		0,0			100,0.4	
E_1/E_2	*UD*	*UD*	*UD*	ND_1	ND_2	*UD*	ND_1	ND_2
5	15.360	18.540	14.110	13.095	14.625	18.079	17.320	17.936
10	12.963	16.609	11.908	10.936	12.087	16.419	15.751	15.935
15	12.011	15.877	11.033	10.071	11.071	15.796	15.163	15.179
20	11.490	15.487	10.555	9.597	10.514	15.465	14.853	14.777
25	11.156	15.241	10.248	9.295	10.157	15.258	14.659	14.526
30	10.922	15.070	10.033	9.084	9.907	15.114	14.526	14.352
35	10.746	14.943	9.871	8.927	9.721	15.007	14.429	14.224
40	10.607	14.844	9.744	8.804	9.575	14.924	14.353	14.125
45	10.494	14.763	9.640	8.706	9.458	14.856	14.293	14.045
50	10.400	14.696	9.553	8.624	9.360	14.800	14.243	13.980
55	10.319	14.639	9.479	8.555	9.277	14.752	14.201	13.924
60	10.248	14.589	9.414	8.495	9.205	14.710	14.165	13.877

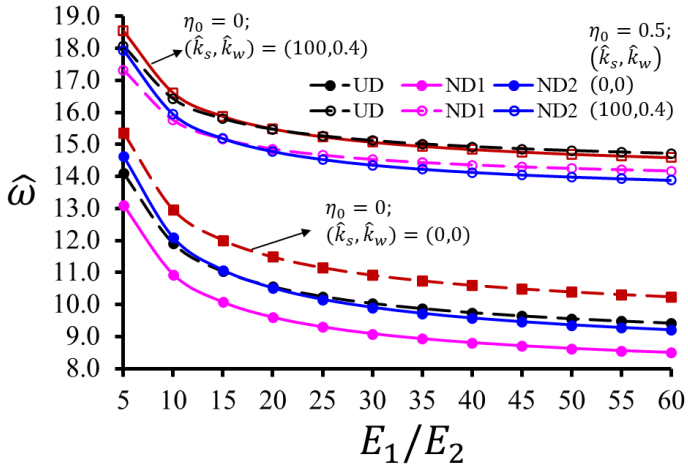

Fig. 7. Variation of non-dimensional fundamental frequency versus in-plane orthotropy ratios

To indicate the effects of the radius-to-curve length ratio on the dimensional fundamental frequency of porous orthotropic cylindrical panel resting on a Pasternak foundation for three porosity patterns, Fig. 8 and Table 5 present the fundamental frequencies versus the radius-to-curve length ratio for both perfect ($\eta_0 = 0$) and porous ($\eta_0 = 0.8$) panels. It is seen that dimensional fundamental frequencies diminish depending on the increasing radius-to-curve length ratios. The difference between *ND*s and *UD* patterns' frequency values increases with an increase in the radius-to-curve length ratio for the Pasternak foundation case. Also, the

difference between ND_1 and ND_2 patterns' frequencies increases depending on the increasing radius-to-curve length ratio for both no foundation and Pasternak foundation cases. With an increasing radius-to-curve length ratio from 0.5 to 5 at no foundation case, the porosity effect increases by (9%) and (13.5%) for ND_1 and ND_2 patterns, respectively. It remains constant at (15.5%) for the UD pattern. With an increasing radius-to-curve length ratio from 0.5 to 5 at the Pasternak foundation case, the porosity effect decreases by (3.5%) and (0.5%) for UD and ND_1 patterns, respectively. It increases by (6.3%) for the ND_2 pattern. With an increasing radius-to-curve length ratio from 0.5 to 5 at the Pasternak foundation case, the ND_1 pattern effect on the fundamental natural frequencies increases by (11%) and (4%) compared to the UD and ND_2 patterns, respectively. Depending on the rising radius-to-curve length ratio from 0.5 to 5, the Pasternak foundation effect on the fundamental natural frequencies increases (17%), (36%), and (23%) for UD, ND_1, and ND_2 patterns, respectively.

Table 5. The effect of R/s ratio on the cylindrical panel's non-dimensional fundamental natural frequency with different foundation parameters, porosity coefficient, and distribution patterns.

	$\eta_0 = 0$		$\eta_0 = 0.8$					
	$\hat{k}_w, \hat{k}_s$							
	0,0	75,0.5	0,0			75,0.5		
R/s	UD	UD	UD	ND_1	ND_2	UD	ND_1	ND_2
0.5	13.141	15.907	11.105	9.930	11.932	15.357	14.638	14.924
1.0	11.232	14.370	9.492	7.813	9.372	14.234	13.293	12.968
1.5	10.842	14.067	9.162	7.355	8.749	14.016	13.029	12.526
2.0	10.702	13.960	9.044	7.187	8.497	13.939	12.935	12.351
2.5	10.636	13.910	8.989	7.108	8.366	13.903	12.892	12.261
3.0	10.601	13.882	8.959	7.065	8.289	13.884	12.868	12.209
3.5	10.579	13.866	8.940	7.039	8.238	13.872	12.854	12.174
4.0	10.565	13.855	8.929	7.022	8.203	13.864	12.844	12.150
4.5	10.556	13.848	8.920	7.010	8.177	13.859	12.838	12.133
5.0	10.549	13.843	8.915	7.002	8.157	13.855	12.833	12.119

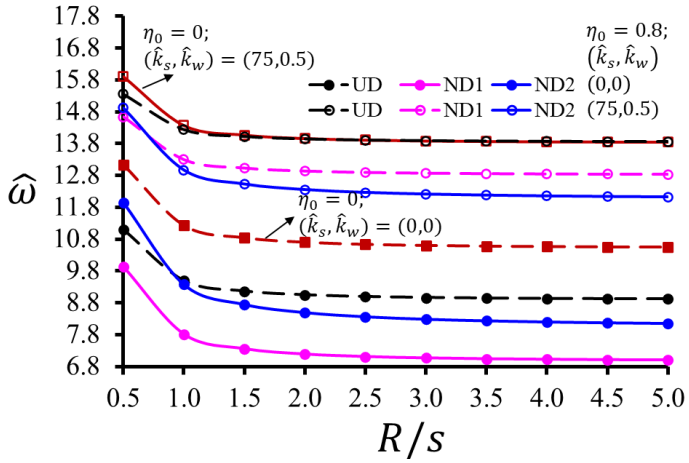

Fig. 8. Variation of non-dimensional fundamental frequency versus radius-to-curve length ratios

5. Conclusions

The paper studies the free vibration of porous orthotropic cylindrical panels resting on an elastic foundation within the higher-order shear deformation theory. Three types of porosity distributions are considered. Mechanical properties of the porous panel are modeled in the thickness direction based on specific functions. The equations of motion are derived by using

Hamilton's principle. The Galerkin solution method is used to solve governing partial differential equations. It is indicated that the vibration responses of porous orthotropic cylindrical panels are significantly affected by various parameters such as elastic foundation stiffness, porosity coefficients, porosity distribution patterns, and geometrical parameters.

This subject is a less-explored area in vibration analysis, and including porosity introduces complexities related to structure-foundation interactions. Incorporating an elastic foundation beneath the panels adds a layer of realism to the analysis. The interaction between the panel and the foundation significantly influences the panel's vibration response, making the study relevant for practical engineering applications. The utilization of shear deformation theory is a distinctive approach. This theory considers the effects of transverse shear deformation, which is particularly important for thin and composite structures like cylindrical panels. Its integration adds precision to the results compared to classical plate theories. This subject bridges structural mechanics, soil-structure interaction, and material science concepts. The novelty lies in combining these diverse fields to analyze a complex system's behavior comprehensively. The outcomes of this study can have implications for various engineering fields, such as aerospace, civil engineering, and mechanical engineering. Optimizing the design of structures with these characteristics could lead to improved performance and efficiency.

Numerical results show that:

- The ND_2 cylindrical panels' dimensional fundamental frequencies are more significant than the ND_1 ones.
- The effect of the ND_1 pattern on the fundamental frequencies is more significant than the other patterns.
- The elastic foundation effect on the fundamental frequencies increases with the rising porosity coefficient.
- The influence of porosity on the dimensionless frequencies decreases with increasing elastic foundation stiffness.
- The effect of porosity on the fundamental frequencies of cylindrical panels resting on the Pasternak foundation decreases with increasing orthotropy and radius-to-curve length ratios for *UD* and ND_1 patterns. It increases for the ND_2 pattern.
- The influence of porosity on the fundamental frequencies of cylindrical panels with no foundation increases with increasing orthotropy and radius-to-curve length ratios for ND_1 and ND_2 patterns. It remains constant for the *UD* pattern.
- The difference between ND_1 and ND_2 cylindrical panels' frequencies increases depending on the increasing radius-to-curve length ratio.

Appendix A

$$\alpha_{31} = K_{12}K_{23}(K_{44}K_{55} - K_{45}K_{54}) + K_{12}K_{43}(K_{25}K_{54} - K_{24}K_{55}) + K_{12}K_{53}(K_{24}K_{45} - K_{25}K_{44}) + K_{13}K_{45}(K_{22}K_{54} - K_{24}K_{52}) + K_{13}K_{44}(K_{25}K_{52} - K_{22}K_{55}) + K_{13}K_{42}(K_{24}K_{55} - K_{25}K_{54}) + K_{14}K_{23}(K_{45}K_{52} - K_{42}K_{55}) + K_{14}K_{22}(K_{43}K_{55} - K_{45}K_{53}) + K_{14}K_{25}(K_{42}K_{53} - K_{43}K_{52}) + K_{15}K_{53}(K_{22}K_{44} - K_{24}K_{42}) + K_{15}K_{43}(K_{24}K_{52} - K_{22}K_{54}) + K_{15}K_{23}(K_{42}K_{54} - K_{44}K_{52}) \quad \text{(A1)}$$

$$\alpha_{32} = -K_{11}K_{23}(K_{44}K_{55} - K_{45}K_{54}) - K_{11}K_{43}(K_{25}K_{54} - K_{24}K_{55}) - K_{11}K_{53}(K_{24}K_{45} - K_{25}K_{44}) - K_{13}K_{45}(K_{21}K_{54} - K_{24}K_{51}) - K_{13}K_{44}(K_{25}K_{51} - K_{21}K_{55}) - K_{13}K_{41}(K_{24}K_{55} - K_{25}K_{54}) - K_{14}K_{23}(K_{45}K_{51} - K_{41}K_{55}) - K_{14}K_{21}(K_{43}K_{55} - K_{45}K_{53}) - K_{14}K_{25}(K_{41}K_{53} - K_{43}K_{51}) - K_{15}K_{21}(K_{44}K_{53} - K_{43}K_{54}) - K_{15}K_{41}(K_{23}K_{54} - K_{24}K_{53}) - K_{15}K_{51}(K_{24}K_{43} - K_{23}K_{44}) \quad \text{(A2)}$$

$$\alpha_{33} = K_{11}K_{22}(K_{44}K_{55} - K_{45}K_{54}) + K_{11}K_{42}(K_{25}K_{54} - K_{24}K_{55}) + K_{11}K_{52}(K_{24}K_{45} - K_{25}K_{44}) + K_{12}K_{21}(K_{45}K_{54} - K_{44}K_{55}) + K_{12}K_{24}(K_{41}K_{55} - K_{45}K_{51}) + K_{12}K_{25}(K_{44}K_{51} - K_{41}K_{54}) + K_{14}K_{41}(K_{25}K_{52} - K_{22}K_{55}) + K_{14}K_{21}(K_{42}K_{55} - K_{45}K_{52}) + K_{14}K_{51}(K_{22}K_{45} - K_{25}K_{42}) + K_{15}K_{41}(K_{22}K_{54} - K_{24}K_{52}) + K_{15}K_{21}(K_{44}K_{52} - K_{42}K_{54}) + K_{15}K_{51}(K_{24}K_{42} - K_{22}K_{44}) \quad \text{(A3)}$$

$$\alpha_{34} = -K_{11}K_{42}(K_{25}K_{53} - K_{23}K_{55}) - K_{11}K_{22}(K_{43}K_{55} - K_{45}K_{53}) - K_{11}K_{52}(K_{23}K_{45} - K_{25}K_{43}) - K_{12}K_{21}(K_{45}K_{53} - K_{43}K_{55}) - K_{12}K_{51}(K_{25}K_{43} - K_{23}K_{45}) - K_{12}K_{41}(K_{23}K_{55} - K_{25}K_{53}) - K_{13}K_{41}(K_{25}K_{52} - K_{22}K_{55}) - K_{13}K_{21}(K_{42}K_{55} - K_{45}K_{52}) - K_{13}K_{51}(K_{22}K_{45} - K_{25}K_{42}) - K_{15}K_{21}(K_{43}K_{52} - K_{42}K_{53}) - K_{15}K_{51}(K_{23}K_{42} - K_{22}K_{43}) - K_{15}K_{41}(K_{22}K_{53} - K_{23}K_{52}) \quad \text{(A4)}$$

$$\alpha_{35} = K_{11}K_{22}(K_{43}K_{54} - K_{44}K_{53}) + K_{11}K_{42}(K_{24}K_{53} - K_{23}K_{54}) + K_{11}K_{52}(K_{23}K_{44} - K_{24}K_{43}) + K_{12}K_{41}(K_{23}K_{54} - K_{24}K_{53}) + K_{12}K_{21}(K_{44}K_{53} - K_{43}K_{54}) + K_{12}K_{51}(K_{24}K_{43} - K_{23}K_{44}) + K_{13}K_{51}(K_{22}K_{44} - K_{24}K_{42}) + K_{13}K_{21}(K_{42}K_{54} - K_{44}K_{52}) + K_{13}K_{41}(K_{24}K_{52} - K_{22}K_{54}) + K_{14}K_{41}(K_{22}K_{53} - K_{23}K_{52}) + K_{14}K_{21}(K_{43}K_{52} - K_{42}K_{53}) + K_{14}K_{51}(K_{23}K_{42} - K_{22}K_{43}) \quad \text{(A5)}$$

References

[1] Pasternak, P.L., On a new method of analysis of an elastic foundation by means of two foundation constants, Gosstroyizdat, Moscow, 1954.

[2] Zamani, H.A., Aghdam, M.M., Sadighi, M., Free vibration analysis of thick viscoelastic composite plates on visco-Pasternak foundation using higher-order theory. *Composite Structures*, 182, 25-35, 2017.

[3] Duc, N.D., Quang, V.D., Anh, V.T.T., The nonlinear dynamic and vibration of the S-FGM shallow spherical shells resting on an elastic foundations including temperature effects. *International Journal of Mechanical Sciences*, 123, 54-63, 2017.

[4] Zenkour, A.M., Radwan, A.F., Free vibration analysis of multilayered composite and soft core sandwich plates resting on Winkler–Pasternak foundations. *Journal of Sandwich Structures & Materials*, 20, 169-190, 2016.

[5] Quan, T.Q., Duc, N.D., Nonlinear vibration and dynamic response of shear deformable imperfect functionally graded double-curved shallow shells resting on elastic foundations in thermal environments. *Journal of Thermal Stresses*, 39, 437-459, 2016.

[6] Park, K.J., Kim, Y.W., Vibration characteristics of fluid-conveying FGM cylindrical shells resting on Pasternak elastic foundation with an oblique edge. *Thin-Walled Structures*, 106, 407-419, 2016.

[7] Ninh, D.G., Bich, D.H., Nonlinear thermal vibration of eccentrically stiffened Ceramic-FGM-Metal layer toroidal shell segments surrounded by elastic foundation. *Thin-Walled Structures*, 104, 198-210, 2016.

[8] Jung, W.Y., Han, S.C., Park, W.T., Four-variable refined plate theory for forced-vibration analysis of sigmoid functionally graded plates on elastic foundation. *International Journal of Mechanical Sciences*, 111, 73-87, 2016.

[9] Kim, Y.W., Free vibration analysis of FGM cylindrical shell partially resting on Pasternak elastic foundation with an oblique edge. *Composites Part B: Engineering*, 70, 263-276, 2015.

[10] Asanjarani, A., Satouri, S., Alizadeh, A., Kargarnovin, M.H., Free vibration analysis of

2D-FGM truncated conical shell resting on Winkler–Pasternak foundations based on FSDT. *Proceedings of the Institution of Mechanical Engineers, Part C: Journal of Mechanical Engineering Science*, 229, 818-839, 2015.

[11] Ahmed, M.K., Effects of non-uniform Winkler foundation and non-homogeneity on the free vibration of an orthotropic elliptical cylindrical shell. *European Journal of Mechanics-A/Solids*, 49, 570-581, 2015.

[12] Bich, D.H., Duc, N.D., Quan, T.Q., Nonlinear vibration of imperfect eccentrically stiffened functionally graded double curved shallow shells resting on elastic foundation using the first order shear deformation theory. *International Journal of Mechanical Sciences*, 80, 16-28, 2014.

[13] Thai, H.-T., Park, M., Choi, D.-H., A simple refined theory for bending, buckling, and vibration of thick plates resting on elastic foundation. *International Journal of Mechanical Sciences*, 73, 40-52, 2013.

[14] Sobhy, M., Buckling and free vibration of exponentially graded sandwich plates resting on elastic foundations under various boundary conditions. *Composite Structures*, 99, 76-87, 2013.

[15] Kamranfard, M., Saidi, A., Naderi, A., Analytical solution for vibration and buckling of annular sectorial porous plates under in-plane uniform compressive loading. *Proceedings of the Institution of Mechanical Engineers, Part C: Journal of Mechanical Engineering Science*, 232, 2211-2228, 2018.

[16] Turan, F., Natural frequencies of porous orthotropic two-layered plates within the shear deformation theory. *CHALLENGE*, 9, 1-11, 2023.

[17] Wang, Y.Q., Electro-mechanical vibration analysis of functionally graded piezoelectric porous plates in the translation state. *Acta Astronautica*, 143, 263-271, 2018.

[18] Rezaei, A., Saidi, A., An analytical study on the free vibration of moderately thick fluid-infiltrated porous annular sector plates. *Journal of Vibration and Control*, 24, 4130-4144, 2018.

[19] Barati, M.R., Zenkour, A.M., Electro-thermoelastic vibration of plates made of porous functionally graded piezoelectric materials under various boundary conditions. *Journal of Vibration and Control*, 24, 1910-1926, 2018.

[20] Barati, M.R., Vibration analysis of porous FG nanoshells with even and uneven porosity distributions using nonlocal strain gradient elasticity. *Acta Mechanica*, 229, 1183-1196, 2018.

[21] Wang, Y., Wu, D., Free vibration of functionally graded porous cylindrical shell using a sinusoidal shear deformation theory. *Aerospace Science and Technology*, 66, 83-91, 2017.

[22] Shojaeefard, M.H., Googarchin, H.S., Ghadiri, M., Mahinzare, M., Micro temperature-dependent FG porous plate: Free vibration and thermal buckling analysis using modified couple stress theory with CPT and FSDT. *Applied Mathematical Modelling*, 50, 633-655, 2017.

[23] Akbaş, Ş.D., Vibration and static analysis of functionally graded porous plates. *Journal of Applied and Computational Mechanics*, 3, 199-207, 2017.

[24] Rezaei, A., Saidi, A., Exact solution for free vibration of thick rectangular plates made of porous materials. *Composite Structures*, 134, 1051-1060, 2015.

[25] Demir, Y., Turan, F., Stability of Porous Orthotropic Cylindrical Panel Resting On Winkler Foundation via Hyperbolical Shear Deformation Theory, in: 10. International Congress of

Academic Research, Bolu, 2023, pp. 124-133.

[26] Kumar, V., Singh, S., Saran, V.H., Harsha, S.P., Vibration characteristics of porous FGM plate with variable thickness resting on Pasternak's foundation. *European Journal of Mechanics-A/Solids*, 85, 104124, 2021.

[27] Tran, T.T., Tran, V.K., Pham, Q.-H., Zenkour, A.M., Extended four-unknown higher-order shear deformation nonlocal theory for bending, buckling and free vibration of functionally graded porous nanoshell resting on elastic foundation. *Composite Structures*, 264, 113737, 2021.

[28] Balak, M., Jafari Mehrabadi, S., Mohseni Monfared, H., Feizabadi, H., Free vibration behavior of an elliptical sandwich microplate, consisting of a saturated porous core and two piezoelectric face layers, standing on an elastic foundation. *Acta Mechanica*, 233, 3253-3290, 2022.

[29] Pham, Q.-H., Tran, T.T., Tran, V.K., Nguyen, P.-C., Nguyen-Thoi, T., Zenkour, A.M., Bending and hygro-thermo-mechanical vibration analysis of a functionally graded porous sandwich nanoshell resting on elastic foundation. *Mechanics of Advanced Materials and Structures*, 29, 5885-5905, 2022.

[30] Shahverdi, H., Barati, M.R., Vibration analysis of porous functionally graded nanoplates. *International Journal of Engineering Science*, 120, 82-99, 2017.

[31] Chen, Z., Qin, B., Zhong, R., Wang, Q., Free in-plane vibration analysis of elastically restrained functionally graded porous plates with porosity distributions in the thickness and in-plane directions. *The European Physical Journal Plus*, 137, 1-21, 2022.

[32] Ebrahimi, F., Dabbagh, A., Taheri, M., Vibration analysis of porous metal foam plates rested on viscoelastic substrate. *Engineering with Computers*, 37, 3727-3739, 2021.

[33] Akhavan, H., Hashemi, S.H., Taher, H.R.D., Alibeigloo, A., Vahabi, S., Exact solutions for rectangular Mindlin plates under in-plane loads resting on Pasternak elastic foundation. Part II: Frequency analysis. *Computational Materials Science*, 44, 951-961, 2009.

[34] Talebizadehsardari, P., Salehipour, H., Shahgholian-Ghahfarokhi, D., Shahsavar, A., Karimi, M., Free vibration analysis of the macro-micro-nano plates and shells made of a material with functionally graded porosity: A closed-form solution. *Mechanics Based Design of Structures and Machines*, 50, 1054-1080, 2022.